

# Inferring the Surface Irradiance from Measurements Made at Depth

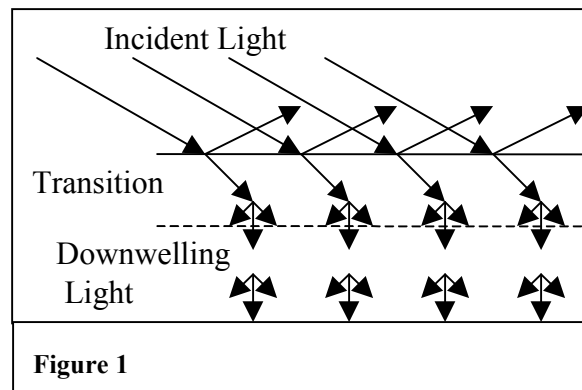
5 Feb 2002

Lotek Wireless Inc.

When doing geolocation based on light measurements made aboard a diving animal, the first step is to infer the surface irradiance from measurements made at depth. The choice of optical pass band strongly affects the complexity of the problem, and a simple model of light absorption can elucidate the effects of various pass band choices.

Choosing a pass band that yields a simple problem leads to algorithms that first determine water properties from a day's light and depth data, then recover an estimate of the surface irradiance during the day. These algorithms are both simple enough and robust enough to be implemented in the measurement platform aboard an animal. We illustrate the effect of algorithm choices using data obtained and processed aboard a free-swimming tuna.

The fate of sunlight incident on the ocean surface may be represented by the diagram at the right. Some fraction is reflected at the surface, the rest is refracted, scattered and finally absorbed in the water below. The diagram neglects diffuse illumination from the sky, waves, ripples, foam and the rest of the interesting detail just at the surface. We note that while the illumination of the surface may be a directed beam (as shown) during the middle of a bright day it will certainly be diffuse both on an overcast day and during sunrise and sunset. Beyond that, this paper will largely neglect detail at and above the surface.



Just below the surface is a transition region in which the light experiences its first few scattering interactions with the water. Despite the sharp line shown dotted in the figure, the transition region actually has an indefinite lower boundary as the light distribution settles toward its asymptotic form.<sup>1</sup> Initially we will also neglect this transition region, except to note that it is likely to be narrower when the incident illumination is diffuse.

Below the transition region lies the relatively orderly regime of downwelling light where many details of the surface illumination and sea state have been smoothed over and lost, and the light is diffuse. Within that regime, animals such as tuna dive and rise experiencing wide excursions in ambient light level. An instrument that is trying to do geolocation from light aboard such an animal must try to remove the effect of depth changes on the total irradiance measured by its light detector. It must infer a value for surface irradiance from the measured irradiance and the measured depth.

### Choice of Detector Properties

We will initially assume that the animal remains within the regime of downwelling light, and in water of uniform properties. Neither assumption is strictly true, and we will eventually need to employ heuristic measures to improve our handling of the situation.

The radiant power  $\Phi$  intercepted by a detector viewing the incident spectral irradiance  $E$  through a filter of response  $A$  is given by<sup>2</sup>

$$\Phi = \int A(\lambda) \cdot E(\lambda) d\lambda \cdot da \quad (1)$$

where the integral extends over the acceptance area of the detector and over all wavelengths for which the integrand is significant. We include the detector spectral response function in  $A(\lambda)$  and take the detector response to be proportional to  $\Phi$ .

To elucidate the effects of several possible filters, in Figure 2 we plot the integrand in Equation 1 vs. wavelength  $\lambda$  for several possible choices of filter pass band. In effect we are assuming that the detector is on (actually just above) the water surface. The red trace represents the spectral response of a typical silicon photodiode multiplied by a simplified version of the solar spectrum.<sup>3</sup> The remaining three traces were obtained by multiplying that product by the pass bands of three candidate optical filters: the blue trace represents a filter centered on 460nm and is intended to represent the response of a particular fluorescent-conversion detector<sup>4</sup> designed to operate in the blue transmission window of the ocean, the green trace represents that same pass band shape translated 50 nm toward longer wavelength, and the magenta trace represents the photopic response centered at 550 nm that is approximated by a number of commercially available filtered silicon photodetectors. All spectra are represented below 800 nm by straight line approximations between values defined at 25nm intervals, plus points at 980, 1100 and 1170 nm in the infrared region where detail is far less important

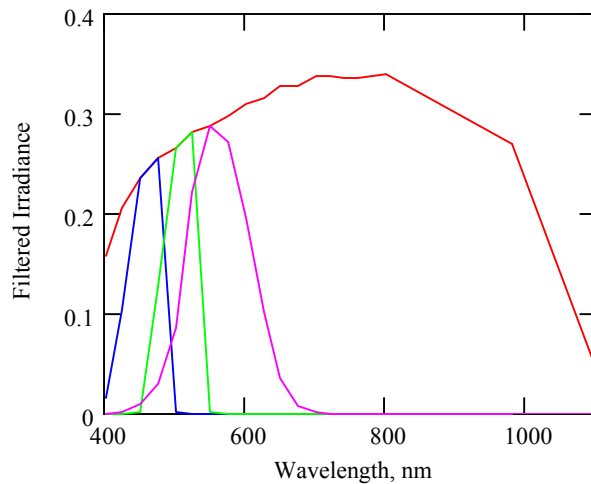


Figure 2: Properties of three filters.

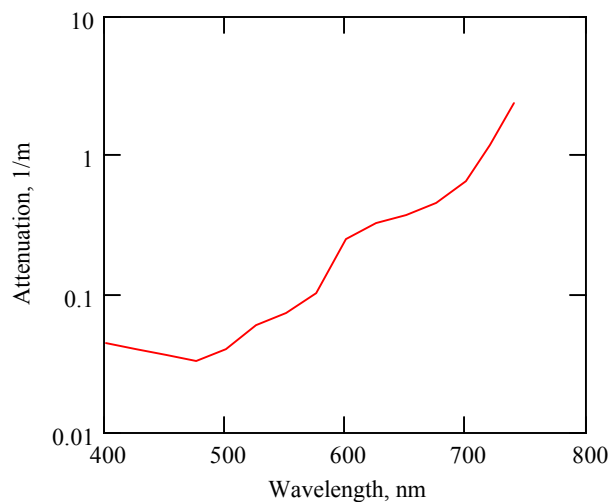


Fig 3: Attenuation of Jerlov IB Water

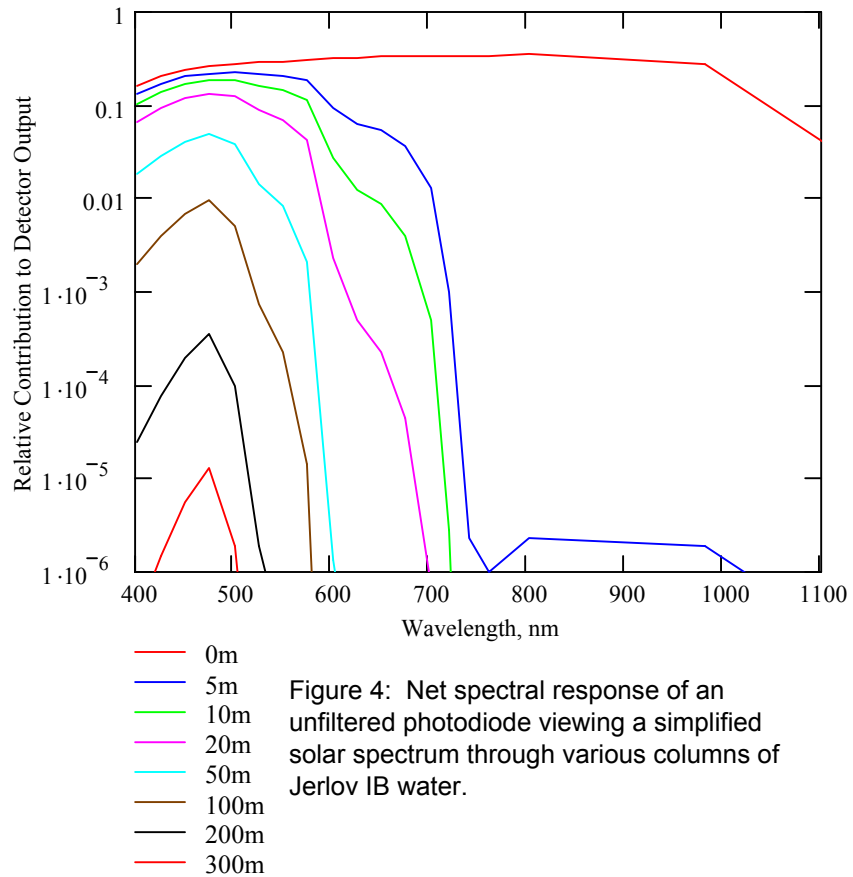
for this work. This admittedly coarse resolution will suffice for the analysis to be done.

Below the transition region, the spectral radiance decays exponentially with depth, a phenomenon that is in this context called Beer's Law. That is, the filtering effect of a water column of length  $d$  is

$$A(\lambda) = \exp(-d \cdot K(\lambda)) \quad (2)$$

where  $K(\lambda)$  is the spectral diffuse attenuation coefficient of the water. We assume for  $K(\lambda)$  the values appropriate to Jerlov type IB water. That choice among Jerlov types results in a net attenuation with depth that is closest to the attenuation actually observed by instruments aboard tuna, though smaller than would be common. The dependence of  $K$  on  $\lambda$  is graphed in figure 3. Since the absorption of Jerlov types is not defined beyond 700 nm, this curve is extended using the absorption properties of pure sea water when displaying spectra over the entire acceptance band of a silicon photodetector.

Multiplying the unfiltered trace of figure 2 by the "filter" defined by the Jerlov attenuation and Beer's law, we can obtain the net response of an otherwise unfiltered silicon detector at various depths below the surface. These traces are shown in figure 4.

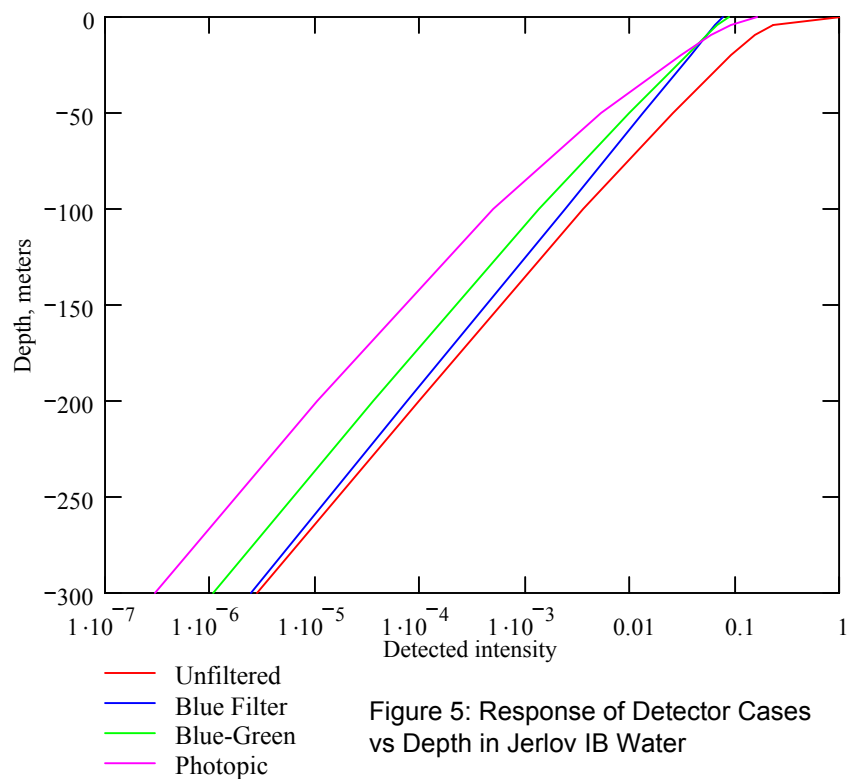


The idea of a "blue window" is clearly illustrated by figure 4. Only a narrow spectral range of blue light survives at depth.

In figure 5 we plot (on a horizontal scale) vs. depth (on the vertical scale) the scalar detector responses of a silicon photodiode filtered as in each of the four cases of figure 2. These values plotted were obtained by trapezoidal rule numerical integration of Equation 1 over the grid used above to define the spectra. Note that in the unfiltered case, the detected intensity drops by more than a factor of 5 in the first 5 meters as most of the red and infrared radiation is absorbed. At depth this response curve approaches that of

the narrow blue filter. At depth most of the remaining light lies near 470nm, and that appropriately filtered detector sees nearly as much light as the unfiltered one.

This blue-filtered case offers another advantage when building a practical instrument: the slope of its response curve is the steepest and the total range of intensities that must be handled is the smallest of the cases considered. The total attenuation range is  $3.2 \times 10^4$  over this 300 m range of depth. This is to be compared with  $5.4 \times 10^5$  for the photopic filter, which is thereby more demanding of the rest of the instrument by a factor greater than ten.



A final advantage to using a narrow filter centered on the transmission window of seawater is that the total detected irradiance also obeys Beer's Law, as indicated by the straightness of the corresponding trace in a semi-log plot vs. depth. This is the key to a simple algorithm for estimating surface intensity.

Under our stated assumptions and with an appropriately chosen filter, the expected dependence of radiant power on depth is a simple exponential. Alternately stated, the dependence of the logarithm of radiant power on depth is the straight line seen in figure 5. Thus it is advantageous to employ a narrow blue filter with a light detector that has an output logarithmic in the detected radiant power. That makes the theoretical dependence of detector output on depth a straight line.

### A Single-Layer Model

The model implied just above is the delightfully simple relation

$$\log(\Phi(0)) = \log(\Phi(d)) + K \cdot d \quad (3)$$

where  $d$  is the depth at which  $\Phi(d)$  was measured, and  $\Phi(0)$  is the inferred radiant power that would have been measured at the surface. The parameter  $K$  is a measure of the

opacity of the water, and the task of fitting this simple model to any given day's data is that of determining the value of K.

Since we must determine K from the same data that is to be corrected, we must identify some feature that will let us separate the power variations due to animal motion from those due to clouds and sunsets, at least in some kind of average sense while fitting the model. The only practically useful distinctions seem to be that 1) the animal ordinarily dives and rises rapidly many times per day while on most days the large changes in illumination at sunrise and sunset are relatively slow and 2) the rapid variations that do occur in surface illumination are only weakly correlated with the animal's excursions in depth while those due to depth are strongly correlated. Thus we can use correlation of rapid variations in the light with rapid variations in depth to fit the model to the water.

In fact, we are again making assumptions that are not entirely justified. Some tuna do habitually make regular dives at sunset and sunrise<sup>5</sup> (as is evident in figure 6) or otherwise swim in response to changes in light intensity, sometimes the animal swimming in shallow water will stay at a constant depth and not explore the water column for us at all, and a partly cloudy day with drifting clouds or a swimming animal can involve rapid changes in surface irradiance. Fortunately there are other features of the situation that tend to come to our rescue. If the animal does not change depth much during a particular day, then there is little depth effect to correct and we do not need a particularly accurate value of K for that day. When the animal is away from the surface, the process of turning incident light into downwelling light will average spatially over surface intensity variations, blurring the sharp edges of cloud shadows. During sunrise and sunset when the most critical measurements must be made for geolocation, the incident illumination is already diffuse and there are no shadows at all. In any case, there appears to be only one practical way to proceed, and it has proven to be reasonably successful.

The simplest available temporal filter that will emphasize rapid variations is the difference of successive measurements. Applying it to equation (3) produces

$$\partial \log(\Phi(0)) = \partial \log(\Phi(d)) + K \cdot \partial d \quad (4)$$

where the difference operator  $\partial$  can represent first, second, etc. differences of successive data items. Experiments with field data suggest that second differences offer no advantage over first differences. In any case, one assumes that the differences of successive values of the surface irradiance are uncorrelated with differences of depth so that  $\partial \log(\Phi(0)) \cdot \partial d$  averages to zero. Then one can sum over all terms of equation 4 for which the light is bright enough to be measured accurately, set the term  $\sum \partial \log(\Phi_i(0)) \cdot \partial d_i$  to zero as just assumed, and solve for K obtaining what amounts to a least-square fit, as

$$K = \frac{-\sum \partial \log(\Phi_i(d)) \cdot \partial d_i}{\sum (\partial d_i)^2} \quad (5)$$

Figure 6 shows a day's field data kindly provided by the National Research Institute of Far Seas Fisheries, Japan<sup>6</sup>. The data were measured on 25 December 1995 aboard a free-swimming juvenile bluefin tuna whose location (as implied by this record and other data returned by the instrument) was in the East China Sea. Values of radiant power and depth were made every 128 seconds, and are shown together with a trace of surface light

intensity inferred in the instrument itself<sup>7</sup> using second differences in equation 5. The light records are expressed on a logarithmic scale of 15 units per decade. Thus the plotted scale range of 0 to 150 corresponds to ten decades of intensity variation. In fact only the top 5.5 decades were active in this tag, and the sudden transition to zero recorded light intensity at the end of the sunrise and sunset curves denotes light judged by the instrument as too dim to be reliably measured.

This record was chosen partly because the behavior of the animal on that particular day presents an uncommonly interesting and illustrative challenge to the single-layer model. The trace of uncorrected light clearly shows variations correlated with depth, being depressed by more than a factor of 100 (35 log units) in the morning when the animal was at depth. That feature has been removed from the corrected trace, which looks much more like traces measured by this kind of tag when moored or on land.

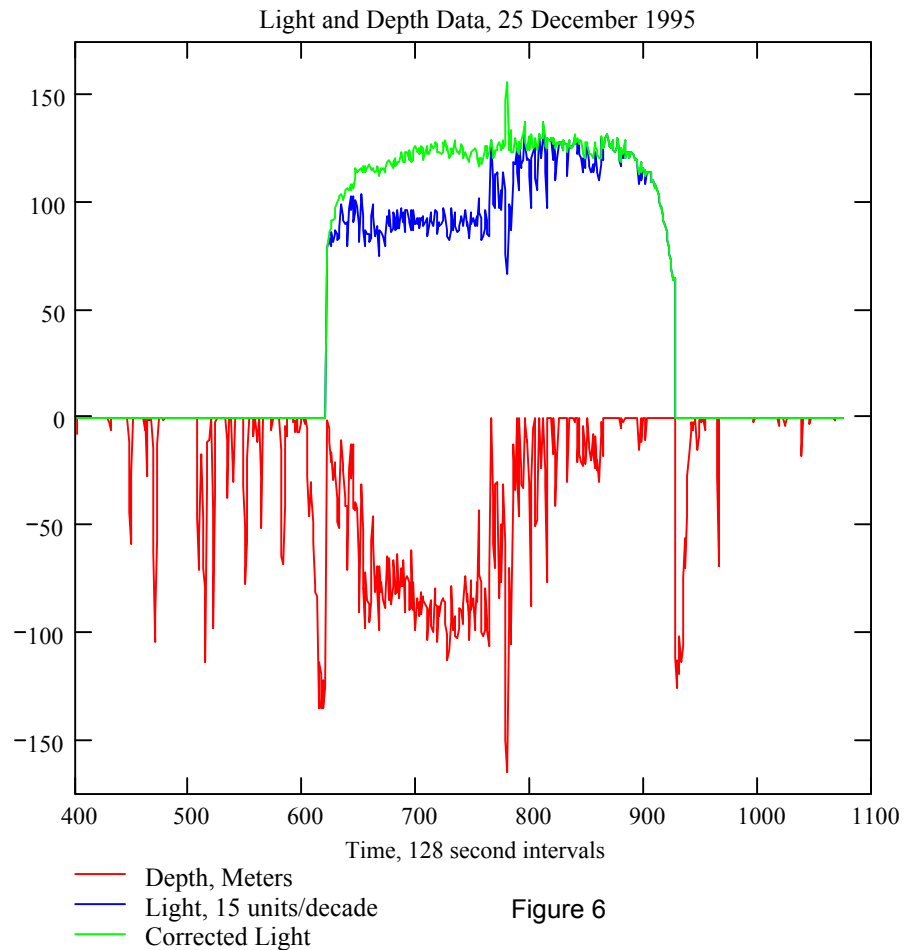


Figure 6

The correction for depth displayed in Figure 6 is good enough to support an entirely serviceable automatic determination of longitude, but it is not perfect. In particular, there is a large upward spike in the corrected light record near midday that is coincident with the deepest dive the animal made that day. As we shall see, it appears to be caused by the tag overcorrecting for that dive by overestimating the attenuation of light in deep water..

## A Two-Layer Model

So far we have ignored the surface transition layer, treating it as if light behaved there in just the same way that it behaves in deeper water. There is ample reason to question this procedure. Not only is the light direction field very different in the two regions, but also the biological load is likely greater in surface water. The presumably spurious spike in the corrected light record of Fig. 6 is additional motivation to now distinguish between surface water and deep water, and treat the two separately.

Accordingly we divide the water column into two layers with a boundary between them at some pre-selected depth  $D_0$ , and we assign separate attenuation constants  $K_u$  for the upper layer and  $K_l$  for the lower one. We define the two functions

$$p(d) = d - D_0 \text{ if } d > D_0, \text{ else } p(d) = 0. \quad (6a)$$

$$n(d) = d \text{ if } d < D_0, \text{ else } n(d) = D_0. \quad (6b)$$

The corresponding two-layer model may be written:

$$\log(\Phi(0)) = \log(\Phi(d)) + K_u \cdot n(d) + K_l \cdot p(d) \quad (7)$$

Making the same assumptions we made previously about the independence of rapid variations in surface illumination and those in swimming depth, a least-squares estimate of the two layer-opacities can be written as the linear system:

$$\begin{aligned} \Sigma(\partial \log(\Phi(d_i)) \partial n(d_i)) + K_u \Sigma(\partial n(d_i))^2 + K_l \Sigma(\partial n(d_i) \partial p(d_i)) &= 0 \\ \Sigma(\partial \log(\Phi(d_i)) \partial p(d_i)) + K_u \Sigma(\partial n(d_i) \partial p(d_i)) + K_l \Sigma(\partial p(d_i))^2 &= 0 \end{aligned} \quad (8)$$

Although substantially more complex than the single-layer case, the calculation needed to apply this two-layer opacity model can still be done in the measurement platform itself. However this model had not been implemented in the instrument that took the field data we are using,

so we must post-process the time series record for the day to demonstrate the effect of this more elaborate model.

Figure 7 compares the uncorrected, single layer, and  $D_0=50\text{m}$  two-layer cases. The model opacity obtained in single layer

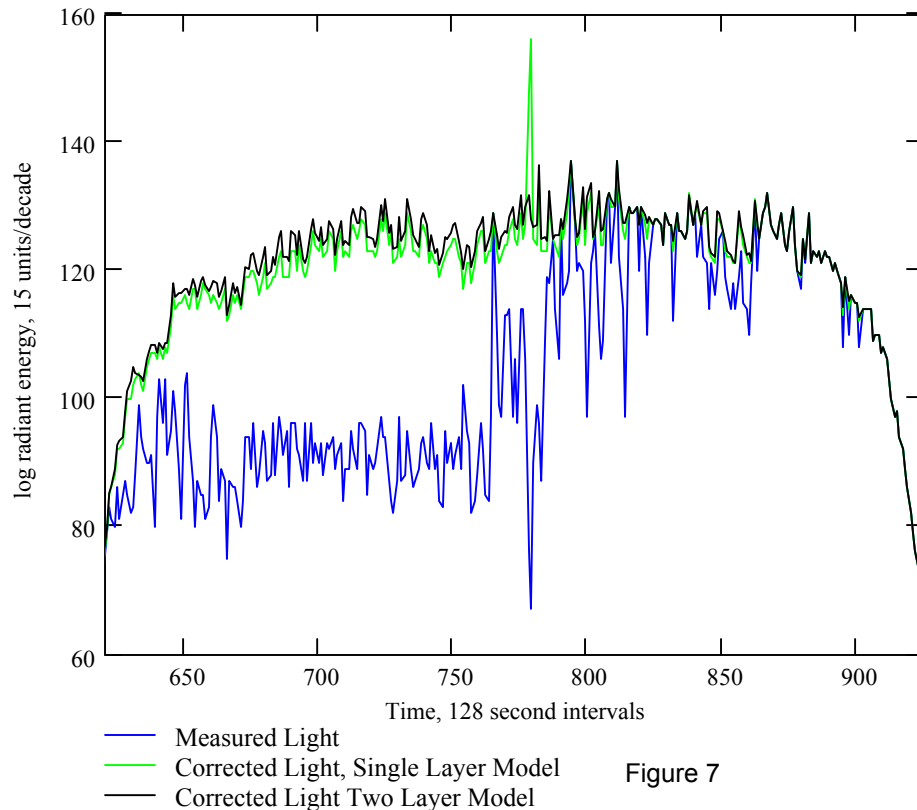


Figure 7

case was  $K=0.381$  log unit/meter, to be compared with the two-layer results  $K_u=0.421$  and  $K_l=0.347$ . (Note that  $15$  log unit/meter = 1 decade/meter, so  $K=0.381$  log unit/meter =  $0.0254$  decade/meter =  $1/(39.4)$  meters/decade.) The two-layer fit found surface-layer opacity greater than that of the single-layer case, and a deep-water opacity that was smaller. All cases investigated show this pattern of values. As a result, the two-layer trace in Figure 7 lies generally higher than the single-layer one, except when the animal enters deep water. The midday spike has disappeared.

It is reasonable to assume that the midday spike was spurious, since it was associated with a depth excursion and is not seen in other records lacking such excursions. By that criterion the two-layer model would seem to be doing a better job, as one might expect. Note that the corrected trace late in the day, when the animal was near the surface and the correction for depth was small, is now actually a bit noisier than the earlier portions that needed correction by a factor of 100 or more (30 or more logarithmic units). Although there is no good way to be certain, it appears that the remaining noise after correction is dominated by other sources such as fluctuations in light incident on the surface and effects of sea state, not by effects of depth.

The choice of  $D_0$  is so far arbitrary; we have developed no criteria for choosing it. Reprocessing the same data with different choices of  $D_0$  suggests that the choice is not especially critical. The value of 50 m used above is somewhere near the center of a wide range of satisfactory values.

### **More layers**

The two-layer model will generalize to a multi-layer model, representing the dependence of the logarithm of detected power upon depth as a broken line with more segments. So long as the segment boundaries are predetermined and not part of the parameter fit, and roughly speaking so long as there are a sufficient number of measurements in each sub-range, one should expect to be able to estimate all parameters from the data. However the requirements for working storage and computation time will increase as the square of the number of segments, and quickly become prohibitive for execution in a miniature instrument.

Even when desktop post-processing provides abundant computational resources, a large number of layers may well not be an advantage. The particular set of depths at which data is available in any given record can strongly affect the conditioning of the linear system in a way that is only roughly captured by the phrase “enough points in each layer”. One must compute and examine a condition number for the relevant matrix. Even in the case of two layers, one must watch for trouble and be ready to default to a coarser model when the data does not robustly determine the parameters of a more complex one. Finally, every added layer uses up a degree of freedom of the data record. Since the assumed independence of light and swimming depth is not exact, our parameter estimates are never perfect. As a result of these two effects, adding layers progressively distorts the record while cleaning it more effectively. As usual, one should make do with the simplest model that will serve, and it appears that the two-layer model serves well.

## Discussion

The choice of a logarithmic detector with its pass band matched to the light spectrum at depth is clearly advantageous, as it both makes best use of detector sensitivity and yields the simplest dependence of detector output on depth. The simplicity of that dependence in the regime of downwelling light suggests first modeling the dependence of radiant power on depth as a single exponential. While that model yields estimates of surface irradiance that are suitable for some purposes, a two-layer model that treats a surface layer separately does a better job and would appear to render an initially overwhelming depth effect negligible when compared with other sources of noise, at least during midday and while the sea surface is illuminated by direct sunlight. While the effects of depth may again become significant during the quieter sunrise and sunset transients, that remains to be investigated.

---

<sup>1</sup>Mobley, Curtis D, *Light and Water*, Academic Press (1994),

<sup>2</sup> Ibid. This reference may be consulted for most details not otherwise footnoted.

<sup>3</sup> *Burle Electro-optics Handbook*, available as a PDF document from [www.burle.com](http://www.burle.com)

<sup>4</sup> As used in the Northwest Marine Technology V1 tags, and the Lotek Wireless LTD2000 series.

<sup>5</sup> Marcinek, Javid J. et al, *Marine Biology* (2001) 138: 869-885

<sup>6</sup> Thanks for permission to use this data are due to Harumi Yamada, Tomoyuki Itoh and other scientists of National Research Institute of Far Seas Fisheries, Japan, whose project deployed the instrument used, a Northwest Marine Technology V1 archival tag.

<sup>7</sup> Strictly speaking, the entire calculation originally done by the instrument was repeated as a post-processing operation for convenience in doing experiments, and the result of that calculation is plotted here. This was possible only because the time series data for some days, including that particular day, were returned along with the opacity constant and geolocation results.